PHYSICAL REVIEW D VOLUME 45, NUMBER 12 15 JUNE 1992

Toward an effective chiral model of high-temperature QCD

Carleton DeTar and Shao-Jing Dong*

Department of Physics, University of Utah, Salt Lake City, Utah 84112

(Received 21 November 1991; revised manuscript received 3 February 1992)

In an effort to expose the mechanism for chiral-symmetry restoration in high-temperature QCD, we use numerical simulations of lattice QCD with staggered fermions to obtain information about possible effective chiral models. We propose the strategy of comparing expressions built from expectation values of low-order polynomials of "macroscopic" meson fields, such as a "Mexican-hat statistic" $\langle\pi^2\sigma\rangle / \langle\pi^2\rangle\langle\sigma\rangle - 1$, computed locally in terms of the quark fields in lattice QCD and in terms of the meson fields in the effective model. We find that, at least at our chosen couplings, QCD behaves like a nonlinear σ model with little change in the local effective potential across the phase transition. This conclusion supports the hypothesis that chiral-symmetry restoration occurs through random fluctuations in a fixed-length order parameter. Included in this work is a thorough test of symmetry breaking and restoration as manifested in the nonlocal staggered chiral fields.

PACS number(s): 12.38.Gc, 11.30.Rd

I. INTRODUCTION

The spontaneously broken $SU(N)\times SU(N)\times U(1)$ chiral symmetry of the strong interactions at low temperature is expected to be restored at high temperature [1]. Indeed, numerical simulations with two and four flavors of staggered fermions have established that at the chiral limit of zero quark mass, QCD undergoes a high-temperature phase transition in which the spontaneously broken chiral symmetry is restored. Evidence for the restoration of chiral symmetry in the high-temperature phase comes both from the vanishing of the order parameter $\langle\bar{\psi}\psi\rangle$ and the formation of chiral multiplets in the various screening channels [2–4]. The simulated chiral symmetry of the staggered fermions is not the full symmetry of the continuous $SU(N)\times SU(N)\times U(1)$ chiral group, but consists of a subgroup with a diagonal $U(1)$ transformation and a set of discrete transformations [5]. It is thought that the simulations will nonetheless approximate the full chiral symmetry in the weak-coupling continuum limit. Indeed, recent simulations show some evidence for flavor-symmetry restoration in the meson spectrum [6].

A long phenomenological tradition describes low-temperature QCD in terms of linear and nonlinear σ models. These models are proposed in order to describe the long-range or low-energy features of QCD, particularly, the light meson sector. A characteristic feature of the linear models is that the effective potential V in the meson field vector (π_i,σ) has a deep minimum at $\pi_i^2+\sigma^2=f_\pi^2$, thereby keeping the fields near this radius. The nonlinear models constrain the fields to this radius. Two important consequences of this constraint are the spontaneous breaking of the symmetry at low temperature and the possibility of topological excitations or Skyrmions. The topological excitations carry baryon number [7].

Experimental efforts to detect the QCD phase transition would be much assisted, if we could identify a clear signal for the formation or decay of the high-temperature phase. It has been suggested that the cooling of a QCD plasma would result momentarily in a disordered orientation of the field vector, necessarily producing topological or baryonic excitations [8]. It has further been suggested that the proliferation of topological excitations may even be the mechanism responsible for chiral-symmetry restoration itself [9]. Thus one may expect that a good signal for the cooling of the QCD plasma would be a copious production of baryons and antibaryons, assuming, of course, that annihilations in the final state do not spoil the effect [10].

Our purpose here is to investigate further the mechanism of chiral-symmetry restoration in QCD, by attempting to use a numerical simulation including dynamical fermions to learn something about the local effective potential in the meson fields at high temperature. Specifically, we ask whether this potential is closer to the Gaussian form

$$V_G(\pi_i,\sigma)=\frac{\mu^2}{2}(\pi_i^2+\sigma^2)+\frac{m^2}{2}\sigma^2 \tag{1}$$

or a more general "bowl" potential

$$V_G(\pi_i,\sigma)=\lambda(\pi_i^2+\sigma^2+f_\pi^2)^2-m\sigma, \tag{2}$$

on the one hand, as suggested by the expected high-temperature global mean-field potential and by many models [11], or closer to the Mexican-hat form

$$V_\sigma(\pi_i,\sigma)=\lambda(\pi_i^2+\sigma^2-f_\pi^2)^2-m\sigma, \tag{3}$$

on the other, as suggested by the low-temperature phenomenological model. If either of the first two expres-

*Present address: Department of Physics and Astronomy, University of Kentucky, Lexington, KY 40506-0055.

sions is closer to the truth, then the phase transition entails a drastic change from the zero-temperature local effective potential, and topological excitations are probably insignificant. If the last, then the phase transition does not change the local effective potential drastically and topological excitations are probably significant.

Before we can proceed, it is necessary to make these ideas more precise, because we are not working with a local meson field theory, but an approximation to QCD. The meson fields are described in QCD as composites of quarks and antiquarks. These fields are to be used in a long-range description of QCD. Therefore, we should treat them as "macroscopic" fields in the sense that they are to be averaged over a small, but finite volume V_x around the point x:

$$\pi_i(x) = i \int_{r \in V_x} dr\, \bar{q}(r)\gamma_5 \tau_i q(r). \tag{4}$$

Averaging over the volume regulates polynomials in the fields. The size of this volume should be small compared with the pion Compton wavelength, but large compared with Compton wavelengths of mesons not included in the effective theory, such as the ρ. As a matter of convenience in the lattice calculations with our choice of gauge coupling, we take this volume to be a single lattice hypercube, but at weaker couplings, it should include more than one hypercube.

It should also be emphasized that we want to determine the *local* effective potential in the macroscopic meson fields and not the more commonly defined global mean-field effective potential. The local potential appears in a phenomenological action together with a kinetic energy term and is used to describe the long-range behavior of the theory. It is "effective" and presumably temperature dependent, because it is an approximation to QCD. Both extreme forms (1),(3) of the local potential lead at high temperature to similar global mean-field potentials with a minimum at the origin. Thus the global mean-field potential does not distinguish the mechanism of the phase transition.

In strong coupling and high dimension Kawamoto and Smit derived an effective meson field theory from lattice QCD with Wilson fermions [12]. They found a potential reminiscent of the linear σ model, but with a logarithmic singularity at the origin. Their methods apply equally to lattices at low and high temperature. However, without prior assumptions about the integration measure of the meson fields, their method does not lead to a unique result. Moreover, it requires approximations. Therefore, we work directly with a numerical simulation. We simply compare numerical results of simulations in QCD with simulations in an effective theory. Quantities to be compared are built from *local* expectation values of low-order polynomials in the macroscopic meson fields:

$$\langle \pi_i(x) \rangle, \langle \sigma(x) \rangle, \langle \pi_i^2(x) \rangle, \langle \sigma^2(x) \rangle, \langle \pi_i^2(x)\sigma(x) \rangle, \text{ etc.} \tag{5}$$

Henceforth we omit explicit reference to the coordinate x. These expectation values suffice for our present purpose, but a more sophisticated approach would also compare calculations of meson propagators. We are particularly interested in a dimensionless "Mexican-hat statistic"

$$P_3(m) = \frac{\langle \pi_i^2 \sigma \rangle - \langle \pi_i^2 \rangle \langle \sigma \rangle}{\langle \pi_i^2 \rangle \langle \sigma \rangle}. \tag{6}$$

Although this statistic is defined for nonzero m, we will often consider the chiral limit $m \to 0$.

How will this observable help to distinguish among the three choices of potential? With the Gaussian form Eq. (1) there is no correlation between the π and σ fields and $P_3 \approx 0$, independent of the symmetry-breaking term m. With the Mexican-hat form (3) and nonzero m the field vector is confined to an arc of radius f_π with minimum at $(f_\pi, 0)$. If σ decreases from its mean value, π_i^2 must increase. Therefore we expect the correlation $P_3 < 0$, with no dramatic dependence on the symmetry-breaking parameter. Indeed, for small fluctuations in the fields, we expect $P_3 \approx -\frac{1}{2}$. In the Appendix we show for the hat shape potential that in lattice mean-field theory in the chiral limit $P_3(0)$ ranges from -0.50 to -0.22 for large values of λ . Naturally, more negative values are associated with stronger coupling. This result is confirmed in our simulation of a realted U(1) chiral model, described in Sec. V. For small values of λ with the hat potential and for all coupling strengths with the bowl potential, Eq. (2), there is correlation between the fields that tends to produce $P_3 < 0$, but only weakly so. In lattice mean-field theory we find that in that case $P_3(0)$ ranges from 0 to -0.22 as λ ranges from large values to 0. Thus only for weak-coupling λ with consequent small magnitudes for $P_3(0)$ is a distinction between the bowl and hat not possible.

We also report results for the fluctuation ratios

$$R = \frac{\langle \pi_i^2 \rangle - \langle \pi_i \rangle^2}{\langle \sigma^2 \rangle - \langle \sigma \rangle^2} \tag{7}$$

although, as we shall see, this statistic does not contrast the various potentials.

In Sec. II we use a toy model to discuss the quantities we are comparing and the problems in defining an effective potential. We discuss the symmetries of the four-flavor staggered action and define the quantities to be measured in Sec. III. In Secs. IV and V we give details and results of the simulations for both QCD and the three-dimensional x-y model that serves as our U(1) analogue. The concluding section gives a discussion and summary of our findings.

II. EFFECTIVE ACTION

In this section we describe a toy model that encapsulates strong-coupling features of the staggered fermion model. We use it to illustrate ambiguities in deriving an effective meson action and to obtain an exact result for the statistics of interest in a simple model.

The model puts spinless SU(2) color Grassmann fields on only two sites, which we call "e" and "o" for even and odd. The action with sources J_e and J_o is just

$$S = \bar{\chi}_e \chi_e J_e + \bar{\chi}_o \chi_o J_o + (\bar{\chi}_e U \chi_o - \bar{\chi}_o U^\dagger \chi_e). \tag{8}$$

The single, nondynamical SU(2) gauge link matrix U turns out to be irrelevant for the local quantities of interest, but the lack of a gauge kinetic energy term is analogous to a strong-coupling approximation. At $J_e = J_o = 0$ the action is symmetric under the U(1)×U(1) chiral transformation

$$\chi_e \to e^{i(\alpha+\beta)}\chi_e, \quad \chi_o \to e^{-i(\alpha-\beta)}\chi_o,$$
$$\bar{\chi}_e \to e^{i(\alpha-\beta)}\bar{\chi}_e, \quad \bar{\chi}_o \to e^{-i(\alpha+\beta)}\bar{\chi}_o. \tag{9}$$

The action can be written as $S = (\bar{\chi}, M\chi)$, where the fermion matrix is

$$M = \begin{pmatrix} J_e & U \\ -U^\dagger & J_o \end{pmatrix}. \tag{10}$$

The chiral pion and σ fields are defined through

$$\pi = i(\bar{\chi}_e\chi_e - \bar{\chi}_o\chi_o)/2, \tag{11}$$

$$\sigma = (\bar{\chi}_e\chi_e + \bar{\chi}_o\chi_o)/2. \tag{12}$$

The generating function is given by

$$Z(J_e, J_o) = \int d\chi_e d\bar{\chi}_e d\chi_o d\bar{\chi}_o dU \exp(S). \tag{13}$$

Up to a constant factor it is

$$Z(J_e, J_o) = \mathrm{Det}\, M = (1 + J_e J_o)^2 . \tag{14}$$

We now attempt to derive an effective meson action by manipulating the integration over the Grassmann variables. We require that the effective action be expressed as an integral over meson fields ϕ_e, to be identified with $\bar{\chi}_e\chi_e$, and ϕ_o, to be identified with $\bar{\chi}_o\chi_o$, with the form

$$Z(J_e, J_o) = \int d\phi_e d\phi_o \exp[S_{\mathrm{eff}}(\phi_e, \phi_o) + J_e\phi_e + J_o\phi_o] . \tag{15}$$

We describe two approaches: one following Kawamoto and Smit [12] and one introducing a delta function.

The first approach writes the generating function as

$$Z(J_e, J_o) = \frac{-1}{4\pi^2} \oint \frac{d\phi_e}{\phi_e} \oint \frac{d\phi_o}{\phi_o} \frac{4 + 2\phi_e\phi_o + \phi_e^2\phi_o^2}{\phi_e^2\phi_o^2} \times \exp(J_e\phi_e + J_o\phi_o), \tag{16}$$

where the contour of integration encircles the origin in the complex ϕ_e and ϕ_o planes.

The second approach introduces delta functions in the form

$$1 = \int d\phi_e d\phi_o \delta(\phi_e - \bar{\chi}_e\chi_e)\delta(\phi_o - \bar{\chi}_o\chi_o), \tag{17}$$

where

$$\delta(\phi_e - \bar{\chi}_e\chi_e) = \frac{1}{2\pi} \int d\lambda_e \exp[i\lambda_e(\phi_e - \bar{\chi}_e\chi_e)], \tag{18}$$

and, after some algebra, writes the generating function as

$$Z(J_e, J_o) = \int d\phi_e d\phi_o \left(1 + \frac{\partial^2}{\partial\phi_e\partial\phi_o}\right)^2 \times \delta(\phi_e)\delta(\phi_o) \exp(J_e\phi_e + J_o\phi_o). \tag{19}$$

Both representations give exactly the same generating function, but the resulting effective action clearly depends on the chosen integration domain and measure. The second choice has a more conventional domain and measure. The peculiar form of the action in either case reflects the underlying fermion character of the composite field. With two colors the Pauli exclusion principle requires that $\langle(\bar{\chi}_e\chi_e)^n\rangle$ vanish for $n > 2$. Thus the generating function must be quadratic in each of the source variables, and the term $\exp(S_{\mathrm{eff}})$ in the first case must have a finite Laurent series expansion, and in the second case, must be a doubly quadratic differential operator acting on a delta function. These peculiarities arise from an attempt to define the pion field precisely locally, and should go away in the continuum limit with a macroscopic definition of the pion field as in Eq. (4).

For these reasons we have chosen a different approach to determining an effective meson action for QCD, namely, of proposing more traditional forms of the effective meson action, and distinguishing among them by requiring that key local macroscopic observables, e.g., those of Eq. (5), have the same value, computed in either language.

A straightforward evaluation with quark mass $J_e = J_o = m$ gives

$$\langle\pi\rangle = 0, \tag{20}$$
$$\langle\sigma\rangle = 2m/(1 + m^2), \tag{21}$$
$$\langle\pi^2\rangle = 1/(1 + m^2), \tag{22}$$
$$\langle\sigma^2\rangle - \langle\sigma\rangle^2 = (1 - m^2)/(1 + m^2)^2, \tag{23}$$
$$\langle\pi^2\sigma\rangle = m/(1 + m^2)^2. \tag{24}$$

So the dimensionless statistics of interest are

$$R = \langle\pi^2\rangle / [\langle\sigma^2\rangle - \langle\sigma\rangle^2] = (1 + m^2)/(1 - m^2), \tag{25}$$
$$P_3 = \langle\pi^2\sigma\rangle / \langle\pi^2\rangle\langle\sigma\rangle - 1 = -\tfrac{1}{2}. \tag{26}$$

We see that the ratio of variances R tends quadratically to 1 as the quark mass is decreased to zero. The Mexican-hat statistic P_3 is constant, independent of m.

III. STAGGERED FERMION SYMMETRIES AND OPERATORS

We now turn to a full treatment of the chiral fields in the four-flavor staggered fermion formalism. We use two alternative definitions of the π and σ fields. The first, the "hypercube" definition, starts from the complete description appropriate to an SU(4)×SU(4)×U(1) chiral symmetry. It is hoped that this symmetry is recovered in the continuum limit. In that limit the hypercube definition is presumably the correct choice. At presently accessible values of the lattice parameters, flavor symmetry is strongly broken, particularly in the pseudoscalar sector [6]. Therefore, we also investigate a vastly simpler "odd-even" definition, based on the single faithfully

represented U(1) subgroup of SU(4)×SU(4)×U(1). This definition is used in the toy model described in the previous section. First we discuss the hypercube definition.

We use the conventions and most of the notation of Kluberg-Stern, Morel, Napoly, and Petersson [13]. The conventional staggered fermion action is written as

$$S(\bar{\chi},\chi,U) = S_F(\bar{\chi},\chi,U) + S_g(U), \tag{27}$$

$$S_F = \frac{1}{2}\sum_r a^3[\,\alpha_\mu(r)\bar{\chi}(r)U_\mu(r)\chi(r+\hat{\mu}) - \alpha_\mu(r-\hat{\mu})\bar{\chi}(r)U_\mu^\dagger(r-\hat{\mu})\chi(r-\hat{\mu})] + ma^4\sum_r \bar{\chi}(r)\chi(r)\ , \tag{28}$$

where $\bar{\chi}$, χ are one-component spinors, the γ matrices are Hermitian unitary matrices,

$$\{\gamma_\mu,\gamma_\nu\} = 2\delta_{\mu,\nu},\quad \gamma_\mu^\dagger = \gamma_\mu, \tag{29}$$

and the Dirac phases are

$$\alpha_1(r) = (-)^{r_2+r_3+r_4},\quad \alpha_2(r) = (-)^{r_3+r_4},$$
$$\alpha_3(r) = (-)^{r_4},\quad \alpha_4(r) = 1. \tag{30}$$

The symmetries of this action are conveniently represented in terms of four-flavor, four-component Dirac spinors $q^{\alpha a}(Y)$, assembled from the sixteen one-component χ spinors on each hypercube Y. To be explicit, let

$$r_\mu = 2Y_\mu + \eta_\mu \tag{31}$$

with $\eta_\mu = 0,1$. Then Kluberg-Stern *et al.* define

$$q^{\alpha a}(Y) = \frac{1}{8}\sum_\eta \Gamma_\eta^{\alpha a} U_\eta(Y)\chi_\eta(Y),$$
$$\bar{q}^{\alpha a}(Y) = \frac{1}{8}\sum_\eta \bar{\chi}_\eta(Y)U_\eta^\dagger(Y)\Gamma_\eta^{*\alpha a},$$

where $\chi_\eta(Y) = \chi(2Y+\eta)$,

$$\Gamma_\eta = \gamma_1^{\eta_1}\gamma_2^{\eta_2}\cdots\gamma_4^{\eta_4}, \tag{32}$$

and $U_\eta(Y)$ is a gauge connection from $2Y$ to $2Y+\eta$ through some path, e.g.,

$$U_\eta(Y) = [U_1(2Y)]^{\eta_1}[U_2(2Y+\eta_1)]^{\eta_2}\cdots[U_4(2Y+\eta_1+\eta_2+\eta_3)]^{\eta_4}. \tag{33}$$

In our calculations we average over a set of paths that preserves rotational invariance. The gauge-invariant action in terms of $\bar{q}$ and q is complicated, but to order a is simply

$$S_F = (2a)^4\sum_{Y\mu}\{\,\bar{q}(Y)(\gamma_\mu\otimes 1)D_\mu q(Y) + m\bar{q}(Y)q(Y) + a[\bar{q}(Y)(\gamma_5^\dagger\otimes t_\mu^\dagger t_5^\dagger)D_\mu^2 q(Y) - \tfrac{1}{4}ig\bar{q}(Y)T_{\mu\nu}F_{\mu\nu}(Y)q(Y)] + O(a^2)\}. \tag{34}$$

The covariant lattice derivative D_μ is constructed as usual from the gauge connection $U_\mu(r) = \exp[ig\int_r^{r+\hat{\mu}} A_\mu(x)dx]$ through

$$D_\mu(Y) = \Delta_\mu + igA_\mu(Y), \tag{35}$$

$$\Delta_\mu F(Y) = \frac{1}{4a}[F(Y+\hat{\mu}) - F(Y-\hat{\mu})]. \tag{36}$$

$F_{\mu\nu}(Y)$ is the covariant gauge field strength, $t_\mu = \gamma_\mu^*$ acts on the flavor space, and $T_{\mu\nu}$ is a tensor:

$$T_{\mu\nu} = (\gamma_\mu - \gamma_\nu)\otimes 1 + \tfrac{1}{2}\gamma_5^\dagger[\gamma_\mu,\gamma_\nu]\otimes(t_\mu + t_\nu)^\dagger t_5^\dagger. \tag{37}$$

Written in this form the symmetries of the action are particularly apparent. In addition to rotations, inversions, and translations by two units, the full SU(4)×SU(4)×U(1)×U(1) chiral and flavor symmetry is manifest in the continuum limit at zero quark mass. As is well known, at finite a, this symmetry is broken, as summarized in the next subsection.

A. Global flavor symmetries

On a finite lattice the symmetries of the action include parity (spatial inversion) and a subgroup of SU(4)×SU(4)×U(1)×U(1), consisting of two continuous and thirty other discrete symmetries [13, 14]. We list them here for later use.

1. *Continuous symmetries*

At zero quark mass the action is symmetric under the global U(1)×U(1) transformation Eq. (9), where χ_e is on an even site and χ_o is on an odd site. In the 16-component spinor language, the two generators of this symmetry are

$$V = 1\otimes 1,\quad A = \gamma_5\otimes t_5,$$

associated with β and α, respectively. Since the first factor in the direct product acts on the Dirac spin index and the second on the flavor index, we see that A does not generate the flavor-singlet U(1) axial symmetry. (That one is generated by $\gamma_5\otimes 1$.) Instead, it generates a U(1) subgroup of the SU(4) axial-vector group. As always, the symmetry is explicitly broken by the quark mass term, and $\langle\bar{\chi}\chi\rangle$ is the order parameter for the spontaneously broken symmetry. The vector U(1) symmetry remains unbroken, of course.

2. *Discrete symmetries*

These symmetries arise from translational invariance modulo the hypercube assignment. They are defined in terms of Table 2 of Ref. [14], reproduced here as Table I. All translations discussed below require a shift in the gauge fields through $U_\mu(n) \to U_\mu(n+\xi)$. The vectorlike symmetries lead to

TABLE I. The correspondences of ξ, T_f, and T'_f from Ref. [5].

ξ	P_v	T_f	T'_f
0	$x+y+z+t$	1	$t_1t_2t_3t_4$
e_4	$x+y+z$	$t_1t_2t_3$	t_4
e_1	$y+z$	$t_2t_3t_4$	t_1
e_2	z	$t_1t_3t_4$	t_2
e_3	0	$t_1t_2t_4$	t_3
e_4+e_1	x	t_1t_4	t_2t_3
e_4+e_2	$x+y$	t_2t_4	t_1t_3
e_4+e_3	$x+y+z$	t_3t_4	t_1t_2
e_1+e_2	y	t_1t_2	t_3t_4
e_1+e_3	$y+z$	t_1t_3	t_2t_4
e_2+e_3	z	t_2t_3	t_1t_4
$e_4+e_1+e_2$	$x+y$	t_3	$t_1t_2t_4$
$e_4+e_1+e_3$	x	t_2	$t_1t_3t_4$
$e_4+e_2+e_3$	$x+y$	t_1	$t_2t_3t_4$
$e_1+e_2+e_3$	y	t_4	$t_1t_2t_3$
$e_4+e_1+e_2+e_3$	$x+z$	$t_1t_2t_3t_4$	1

$$\chi(x)\to(-1)^{P_v}\chi(x+\xi),$$
$$\bar{\chi}(x)\to(-1)^{P_v}\bar{\chi}(x+\xi). \tag{38}$$

The axial-vector-like symmetries hold at zero quark mass:

$$\chi(x)\to i(-1)^{P_a}\chi(x+\xi), \tag{39}$$

$$\bar{\chi}(x)\to i(-1)^{P_a}\bar{\chi}(x+\xi); \tag{40}$$
$$P_a=t+x+y+z-P_v.$$

In the 16-component language these symmetry transformations are

$$q\to i1\otimes T_f q \quad \text{(vectorlike)}, \tag{41}$$
$$q\to i\gamma_5\otimes T'_f q \quad \text{(axial-vector-like)}. \tag{42}$$

B. Chiral meson operators and their transformations

Under spatial inversion, of course, all pseudoscalar fields change sign. The flavor transformations are as follows.

1. *Chiral meson operators for SU(4)×SU(4)*

The N-flavor generalization of the chiral scalar fields (π,σ) defines

$$\sigma=\bar{\psi}\psi,$$
$$\pi^i=i\bar{\psi}\gamma_5\lambda^i\psi, \tag{43}$$

where λ^i are generators of SU(N), obeying

$$\left[\frac{\lambda_i}{2},\frac{\lambda_j}{2}\right]=if_{ijk}\frac{\lambda_k}{2},\quad \left\{\frac{\lambda_i}{2},\frac{\lambda_j}{2}\right\}=d_{ijk}\frac{\lambda_k}{2}+\frac{\delta_{ij}}{2}.$$

For groups SU(N) with $N\geq 3$ the anticommutator includes nontrivial d structure constants, requiring N^2 additional fields

$$\tilde{\sigma}=i\bar{\psi}\gamma_5\psi,$$
$$\tilde{\pi}^i=-\bar{\psi}\lambda^i\psi, \tag{44}$$

to obtain closure under the action of the chiral group. Thus for $N=4$ we require 32 real scalar meson fields (half of them scalars and half, pseudoscalars) to generalize the Gell-Mann–Lévy model [15]. In other words, SU(4)×SU(4) $\subset$ O(32). Thus the combination $\sigma^2+\sum(\pi^i)^2+\tilde{\sigma}^2+\sum(\tilde{\pi}^i)^2$ is invariant.

For staggered lattice fermions the 32 fields can be defined as

$$\sigma=\bar{q}q,\quad \pi_a=i\bar{q}\gamma_5\otimes t_a q, \tag{45}$$

$$\tilde{\sigma}=i\bar{q}\gamma_5\otimes 1q,\quad \tilde{\pi}_a=-\bar{q}\,1\otimes t_a q. \tag{46}$$

With the identifications $\pi_1\equiv\sigma$ and $\tilde{\pi}_1\equiv\tilde{\sigma}$, the definitions can be read from Table II. The index a can be associated with a hypercube offset η_a or $\eta_{\bar{a}}$. If these fields are rewritten in terms of the single component χ's, they are linear combinations of $\bar{\chi}(\eta')\chi(\eta)$ with $\eta'=(\eta+\eta_a)\bmod 2$ for scalar fields and $\eta'=(\eta+\eta_{\bar{a}})\bmod 2$, for pseudoscalar fields. The expressions are lengthy and are not reproduced here. In some cases the offsets involve one unit in Euclidean time. Golterman [17] prefers to define all of the scalar-meson states so that no displacement in time is involved, an approach that is appropriate for determining a meson spectrum. Our definitions are more closely related to the continuum expressions and close under the lattice chiral group.

TABLE II. Notation for defining scalar meson fields.

a	η_a	t_a	$\bar{a}$	Even/odd
1	(0,0,0,0)	1	16	e
2	(0,0,0,1)	γ_4	15	o
3	(0,0,1,0)	γ_3	14	o
4	(0,1,0,0)	γ_2	13	o
5	(1,0,0,0)	γ_1	12	o
6	(0,0,1,1)	$\gamma_3\gamma_4$	11	e
7	(0,1,0,1)	$\gamma_2\gamma_4$	10	e
8	(0,1,1,0)	$\gamma_2\gamma_3$	9	e
9	(1,0,0,1)	$\gamma_1\gamma_4$	8	e
10	(1,0,1,0)	$\gamma_1\gamma_3$	7	e
11	(1,1,0,0)	$\gamma_1\gamma_2$	6	e
12	(0,1,1,1)	$\gamma_2\gamma_3\gamma_4$	5	o
13	(1,0,1,1)	$\gamma_1\gamma_3\gamma_4$	4	o
14	(1,1,0,1)	$\gamma_1\gamma_2\gamma_4$	3	o
15	(1,1,1,0)	$\gamma_1\gamma_2\gamma_3$	2	o
16	(1,1,1,1)	$\gamma_1\gamma_2\gamma_3\gamma_4$	1	e

2. *Transformation laws*

Under the continuous vector symmetry transformation $e^{-i\beta 1\otimes 1}$ all mesons fields are invariant. Under an infinitesimal axial-vector-symmetry transformation $1-$

$i\gamma_5 \otimes t_5\alpha$ only fields with a even and $a = 1$ transform nontrivially:

$$\sigma \to \sigma - 2\pi_{16}\alpha, \tag{47}$$

$$\pi_a \to \begin{cases} i\bar{q}\gamma_5 t_a q + 2\bar{q}q\alpha = \pi_a + 2\sigma\alpha, & a = 16, \\ i\bar{q}\gamma_5 t_a q + 2\bar{q}t_a t_5 q\alpha = \pi_a - 2\tilde{\pi}_{\bar{a}}\alpha, & a = \text{even}, \\ i\bar{q}\gamma_5 t_a q = \pi_a, & a = \text{odd}, \end{cases} \tag{48}$$

$$\tilde{\sigma} \to \tilde{\sigma} - 2\tilde{\pi}_{16}\alpha, \tag{49}$$

$$\tilde{\pi}_a \to \begin{cases} -\bar{q}t_a q + 2i\bar{q}\gamma_5 q\alpha = \tilde{\pi}_a + 2\tilde{\sigma}\alpha, & a = 16, \\ -\bar{q}t_a q + 2i\bar{q}\gamma_5 t_a t_5 q\alpha = \tilde{\pi}_a + 2\pi_{\bar{a}}\alpha, & a = \text{even}, \\ -\bar{q}t_a q = \tilde{\pi}_a, & a = \text{odd}. \end{cases} \tag{50}$$

Under the discrete vectorlike transformations the meson fields are invariant or change sign, as follows. Referring to Table I, we associate the flavor transformation iT_f with a hypercube coordinate η_b according to $T_f = t_b = t_1^{\eta_{1b}} t_2^{\eta_{2b}} t_3^{\eta_{3b}} t_4^{\eta_{4b}}$. Then under this symmetry transformation

$$\begin{aligned} &\sigma \to \sigma, \quad \pi_a \to (-)^{\ell_{ab}}\pi_a, \\ &\tilde{\sigma} \to \tilde{\sigma}, \quad \tilde{\pi}_a \to (-)^{\ell_{ab}}\tilde{\pi}_a, \end{aligned} \tag{51}$$

where

$$\ell_{ab} = \eta_a \cdot \eta_b + \sum \eta_{a\mu} \sum \eta_{b\mu}.$$

Similarly under the discrete axial-vector-like transformations $i\gamma_5 T_f'$ the fields also remain invariant or change sign as

$$\begin{aligned} &\sigma \to -\sigma, \quad \pi_a \to (-)^{1+\ell_{ab}}\pi_a, \\ &\tilde{\sigma} \to -\tilde{\sigma}, \quad \tilde{\pi}_a \to (-)^{1+\ell_{ab}}\tilde{\pi}_a. \end{aligned} \tag{52}$$

3. *Effect of symmetries upon operator expectation values*

Parity. Spatial inversion symmetry requires that

$$\langle \pi_a \rangle = \langle \tilde{\sigma} \rangle = 0 \ . \tag{53}$$

Continuous axial-vector symmetry. For the fields transforming nontrivially, as $m \to 0$ we have

$$\langle \sigma \rangle = \langle \tilde{\sigma} \rangle = \langle \pi_a \rangle = \langle \tilde{\pi_a} \rangle = 0 \tag{54}$$

for *even* a and the quantum fluctuations of fields in the same multiplet must be equal:

$$\begin{aligned} &\lim_{m\to 0} \frac{\langle \pi_{16}(Y)^2 \rangle - \langle \pi_{16}(Y) \rangle^2}{\langle \sigma(Y)^2 \rangle - \langle \sigma(Y) \rangle^2} = 1; \\ &\lim_{m\to 0} \frac{\langle \pi_a(Y)^2 \rangle - \langle \pi_a(Y) \rangle^2}{\langle \tilde{\pi}_{\bar{a}}(Y)^2 \rangle - \langle \tilde{\pi}_{\bar{a}}(Y) \rangle^2} = 1 \quad \text{for } a \text{ even}; \\ &\lim_{m\to 0} \frac{\langle \tilde{\pi}_{16}(Y)^2 \rangle - \langle \tilde{\pi}_{16}(Y) \rangle^2}{\langle \tilde{\sigma}(Y)^2 \rangle - \langle \tilde{\sigma}(Y) \rangle^2} = 1. \end{aligned} \tag{55}$$

Discrete symmetries. Fields odd under these symmetries must vanish. Thus if all of the vectorlike symmetries hold, we have

$$\langle \pi_a \rangle = \langle \tilde{\pi}_a \rangle = 0 \ \text{ for all } a \neq 1. \tag{56}$$

If all of the axial-like symmetries hold at zero quark mass we have $\langle \sigma \rangle = \langle \tilde{\sigma} \rangle = \langle \pi_a \rangle = \langle \tilde{\pi}_a \rangle = 0$ in the limit $m \to 0$ for all a.

C. The odd-even construction

This definition is analogous to that of the toy model of Sec. II. The lattice is classified on an odd-even checkerboard and a single π and a σ field are defined as Eq. (12). These fields are analogous to the local hypercube fields σ and π_{16}:

$$\sigma = \frac{1}{16}\sum_{i\eta} (\bar{\chi}_\eta^i \chi_\eta^i), \tag{57}$$

$$\pi_{16} = \frac{1}{16}\left(\sum_{i,\eta=\text{even}} \bar{\chi}_\eta^i \chi_\eta^i - \sum_{i',\eta=\text{odd}} \bar{\chi}_\eta^{i'} \chi_\eta^{i'} \right), \tag{58}$$

and become equivalent to them in the continuum limit. The pair of odd-even scalar fields transform like the hypercube scalar fields σ and π_{16} under the symmetry group. Thus, in particular, they realize the same U(1) subgroup of axial SU(4).

D. Correlation functions

Expectation values of the meson fields and their correlations are computed as usual from the Matthews-Salam formula. Thus, for example, defining the usual fermion matrix through

$$S_F = \sum_{i,j} \bar{\chi}_i M_{ij}(U) \chi_j, \tag{59}$$

we have the quark propagator

$$\int d\bar{\chi}\, d\chi\, dU\, \chi_j \bar{\chi}_i e^{-S(\bar{\chi},\chi,U)} = \int dU\, M_{ji}^{-1}(U) \det M(U) e^{-S_g(U)} \tag{60}$$

and the six-point function

$$\begin{aligned} \int d\bar{\chi}\, d\chi\, dU\, \bar{\chi}_i \chi_j \bar{\chi}_k \chi_l \bar{\chi}_m \chi_n\, e^{-S(\bar{\chi},\chi,U)} = \int dU e^{-S_g(U)} \big(& M_{ji}^{-1} M_{lk}^{-1} M_{nm}^{-1} - M_{jk}^{-1} M_{li}^{-1} M_{nm}^{-1} \\ & + M_{jm}^{-1} M_{li}^{-1} M_{nk}^{-1} - M_{ji}^{-1} M_{lm}^{-1} M_{nk}^{-1} \\ & + M_{jk}^{-1} M_{lm}^{-1} M_{ni}^{-1} - M_{jm}^{-1} M_{lk}^{-1} M_{ni}^{-1} \big) \det M. \end{aligned}$$

From these expressions and Table II we see that to compute expectation values of the meson fields requires calculating the quark propagator between all pairs of points within a hypercube, forming the appropriate linear combinations, and averaging over gauge field configurations. Gauge invariance of the quark propagators is implemented as in Eq. (33), except that to maintain Euclidean invariance, we average over four such choices of path, taking cyclic permutations of the directions ($xyzt$). Calculating the higher moments of the meson fields simply requires forming combinations of products of the same set of quark propagators.

All expectation values require averaging over the fermion fields and gauge fields. It is sometimes helpful to distinguish these two steps explicitly as

$$\langle O \rangle = \left\langle \langle O \rangle_f \right\rangle_g . \tag{61}$$

Then correlations of operators receive two contributions, two steps as follows:

$$\langle O_1 O_2 \rangle - \langle O_1 \rangle \langle O_2 \rangle = \left(\left\langle \langle O_1 O_2 \rangle_f - \langle O_1 \rangle_f \langle O_2 \rangle_f \right\rangle_g \right) + \left(\left\langle \langle O_1 \rangle_f \langle O_2 \rangle_f \right\rangle_g - \langle O_1 \rangle \langle O_2 \rangle \right) . \tag{62}$$

The first term in parentheses involves combinations of inverse matrices forming a single closed fermion world line (color connected), and the second involves products of two or more such world lines (color disconnected). For the operators we consider the second term turns out to be considerably smaller than the first.

E. Coarse lattice suppression

The expressions for the various moments of interest become quite lengthy for the hypercube definition. We give two of the simpler expressions:

$$\langle \pi_{16}^2 \rangle_f - \langle \pi_{16} \rangle_f^2 = -\frac{1}{16^2} \sum_{\eta\eta'} (-)^{\eta+\eta'} \operatorname{Tr}(M_{\eta\eta'} M_{\eta'\eta}), \tag{63}$$

$$\langle \pi_{16}^2 \sigma \rangle_f - \langle \pi_{16}^2 \rangle_f \langle \sigma \rangle_f = -\frac{2}{16^3} \sum_{\eta\eta'\eta''} (-)^{\eta'+\eta''} \operatorname{Re} \operatorname{Tr} \left(M_{\eta\eta'}^{-1} M_{\eta'\eta''}^{-1} M_{\eta''\eta}^{-1} \right) , \tag{64}$$

where the traces are over color only and

$$(-)^{\eta} = (-)^{\sum \eta_\mu} .$$

For the odd-even fields we have

$$\langle \sigma^2 \rangle_f - \langle \sigma \rangle_f^2 = \tfrac{1}{2} [\operatorname{Tr}(M_{ee}^{-1} M_{ee}^{-1}) + \operatorname{Tr}(M_{eo}^{-1} M_{oe}^{-1})], \tag{65}$$

$$\langle \pi^2 \rangle_f - \langle \pi \rangle_f^2 = \tfrac{1}{2} [\operatorname{Tr}(M_{eo}^{-1} M_{eo}^{-1}) - \operatorname{Tr}(M_{ee}^{-1} M_{ee}^{-1})], \tag{66}$$

$$\langle \pi^2 \sigma \rangle_f - \langle \pi^2 \rangle_f \langle \sigma \rangle_f = \tfrac{1}{2} [\operatorname{Tr}(M_{oe}^{-1} M_{eo}^{-1} M_{oo}^{-1}) - \operatorname{Tr}(M_{ee}^{-1} M_{ee}^{-1} M_{ee}^{-1})]. \tag{67}$$

Not surprisingly, the pair Eqs. (63) and (66) and Eqs. (64) and (67) are similar. The only difference is that the odd-even expressions involve only a nearest-neighbor pair, whereas the hypercube expressions involve a sum over pairs selected from all 16 sites in the hypercube. On a coarse lattice this difference leads to a suppression in the hypercube value for the Mexican-hat statistic P_3. Since our main conclusion hinges on the value of P_3, let us take some care to estimate this suppression. On a finite lattice we estimate that the contribution from more distant terms is suppressed by approximately $\exp(-ma)$ for each lattice link of separation, where ma is a typical meson mass. For the gauge couplings of our simulation, ma is of order 1. In the continuum limit $ma \to 0$ and propagation to these slightly more distant points makes little difference. Let us use this rule to estimate the coarse lattice suppression of the hypercube correlation relative to the odd-even correlation. To this end, we organize the sum of terms in Eqs. (63) and (64) according to the distance of propagation:

$$\langle \pi_{16}^2 \rangle_f - \langle \pi_{16} \rangle_f^2 = -\tfrac{1}{16} \left[\operatorname{Tr}(M_{ee}^{-1} M_{ee}^{-1}) - 8 \operatorname{Tr}(M_{eo}^{-1} M_{eo}^{-1}) + \cdots \right] , \tag{68}$$

$$\langle \pi_{16}^2 \sigma \rangle_f - \langle \pi_{16}^2 \rangle_f \langle \sigma \rangle_f = -\tfrac{1}{128} \left[\operatorname{Tr}(M_{ee}^{-1} M_{ee}^{-1} M_{ee}^{-1}) - 8 \operatorname{Tr}(M_{oe}^{-1} M_{eo}^{-1} M_{oo}^{-1}) + \cdots \right] , \tag{69}$$

$$\langle \sigma \rangle_f = \operatorname{Tr} M_{ee}^{-1},$$

where we have used translational and rotational invariance to equate terms calculated from different origins. The omitted terms represent propagation to more distant sites. If we now drop those terms, ignore the color disconnected contributions [from the second pair of parentheses in Eq. (62)] and estimate that in each case the second term in the sum is $\exp(-ma)$ times the first, then we obtain

$$P_{3,\text{hypercube}} \approx \tfrac{1}{8} P_{3,\text{odd-even}} . \tag{70}$$

Below we will see to what extent this estimate is confirmed in our calculations.

IV. QCD SIMULATIONS

A. Parameters

The Monte Carlo simulations were carried out using a hybrid microcanonical algorithm for staggered dynamical fermions with a lattice QCD action [16]. We work on a $10^3 \times 6$ lattice at a temperature near the phase transition. The measurements were made at two gauge couplings β, namely, $\beta = 5.10, 5.25$. In the limit of small quark mass, the first value of β is expected to lie in the low-temperature ($T < T_c$) phase, and the second one in the high-temperature ($T > T_c$) phase [3]. For each β we simulate at four values of the bare quark mass, namely, $m = 0.100$, 0.075, 0.050, 0.025, and for $\beta = 5.25$ at a fifth value $m = 0.0125$. Table III shows the parameter values and extent of the data sample for the simulation. Shown are values of the quark mass m, microcanonical time step dt, gauge coupling β, time to equilibrium in sweeps $n_{\rm eq}$, fermion and gauge field refreshing interval in sweeps n_f and n_g, conjugate-gradient residual tolerance for the microcanonical step and the propagator calculations $r_{\rm mc}$, r_p, the number of iterations between measurements N_m, the number of measurements $N_{\rm fluc}$ of variances such as $\langle \pi_a^2 \rangle$, the number of measurements $N_{\pi a}$ of expectation values of the individual meson fields, such as $\langle \pi_a \rangle$, and the total number of microcanonical time steps $N_{\rm tot}$. No difference was observed when we changed the refreshing interval n_f or n_g from 15 to 50. Our criterion for equilibrium was that the order parameter $\langle \bar{\chi}\chi \rangle$ should approach an apparently steady value up to random fluctuations. The measurement interval was optimized after estimating the decorrelation time. The latter was found from the behavior of the order parameter $\langle \bar{\chi}\chi \rangle$ in a simulation of 3000 iterations after apparent equilibrium.

B. The averaged meson fields and fluctuations

First we report results using the hypercube definition of the fields. Results for averaged meson fields $\langle \sigma \rangle$, $\langle \pi_a \rangle$, $\langle \tilde{\sigma} \rangle$, and $\langle \tilde{\pi_a} \rangle$ are shown in Figs. 1 and 2 and Table IV. The errors are calculated using the standard autocorrelation cutoff formula,

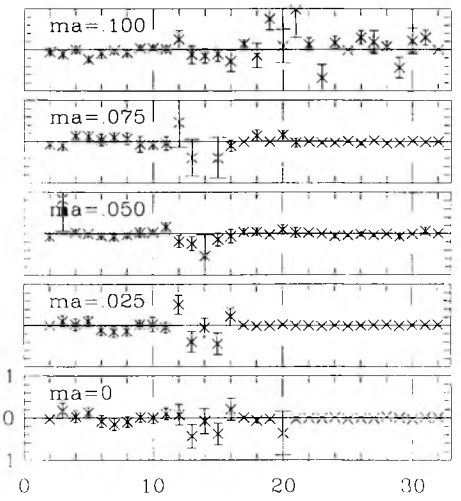

FIG. 1. Expectation value of various hypercube meson fields at $\beta = 5.10$ vs operator index. The ith operator is π_i for $i = 1, 2 \ldots, 16$ and is $\tilde{\pi}_{i-16}$ for $i = 17, \ldots, 32$. The expectation value of the $i = 1$ operator, the σ meson, is given separately in Table IV. All values should be multiplied by 10^{-2}.

$$\Delta\langle O \rangle = \left\{ \frac{\sigma_o^2}{N-1} \left(1 + 2 \sum_{i=1}^{k} \rho_i \right) \right\}^{1/2},$$
$$\sigma_o^2 = \frac{1}{N} \sum_{j=1}^{N} (O_j - \langle O \rangle)^2, \tag{71}$$
$$\rho_i = \frac{1}{\sigma_o^2 (N-i)} \sum_{j=1}^{N-i} (O_j - \langle O \rangle)(O_{j+i} - \langle O \rangle).$$

The cutoff k was selected to keep $\rho_i \geq 0$. The result of a (3,2) Padé extrapolation to the zero quark mass limit is also shown. It is apparent that within the statistical errors, the values of all meson fields, except $\langle \sigma \rangle$, are consistent with zero at all quark masses and at both temperatures.

Results for the ratios of fluctuations of the eight meson pairs that are related under the continuous axial chiral transformations and for the correlation P_3 are shown in

TABLE III. The Monte Carlo simulation parameters.

m	0.100		0.075		0.050		0.025		0.0125
dt	0.02		0.02		0.02		0.01		0.01
β	5.25	5.10	5.25	5.10	5.25	5.10	5.25	5.10	5.25
$n_{\rm eq}$	8000	8000	8000	8000	8000	8000	8000	8000	12000
n_f	30	30	30	30	30	30	30	30	25
n_g	37	37	37	37	37	37	37	37	25
$r_{\rm mc} \times 10^4$	2	2	5	5	5	5	5	5	5
$r_p \times 10^4$	1	1	2	2	2	2	2	2	2
N_m	50	50	100	100	100	100	200	200	250
$N_{\rm fluc}$	550	241	201	119	111	301	160	161	433
$N_{\pi a}$	550	241	327	284	311	301	461	212	433
$N_{\rm tot}$	35500	20050	60800	36400	39100	38100	100200	66400	120250

TABLE IV. Expectation values of σ at two values of β for various quark masses. The zero mass value is found by extrapolation.

β	0.100	0.075	0.050	0.025	0.0125	0.00
5.10	1.061(16)	0.954(12)	0.853(18)	0.591(16)		0.33(2)
5.25	0.770(12)	0.635(9)	0.390(5)	0.199(2)	0.1036(10)	0.002(5)

TABLE V. The ratios of hypercube meson field fluctuations at $\beta = 5.10$. The notation $\langle\sigma^2\rangle_c$ means $\langle\sigma^2\rangle - \langle\sigma\rangle^2$.

m	0.100	0.075	0.050	0.025	0.00
$\langle\pi_{16}^2\rangle / \langle\sigma^2\rangle_c$	4.1(1)	3.12(8)	2.41(5)	1.61(4)	1.54(4)
$\langle\pi_6^2\rangle / \langle\tilde{\pi}_{11}^2\rangle$	35(10)	6.8(5)	3.5(1)	1.69(6)	1.07(8)
$\langle\pi_7^2\rangle / \langle\tilde{\pi}_{10}^2\rangle$	102(91)	7.9(7)	3.7(2)	1.73(6)	1.02(9)
$\langle\pi_8^2\rangle / \langle\tilde{\pi}_9^2\rangle$	39(14)	6.9(5)	3.5(1)	1.69(6)	1.06(8)
$\langle\pi_9^2\rangle / \langle\tilde{\pi}_8^2\rangle$	35(12)	6.8(5)	3.5(1)	1.69(5)	1.07(7)
$\langle\pi_{10}^2\rangle / \langle\tilde{\pi}_7^2\rangle$	89(72)	7.9(7)	3.7(2)	1.73(6)	1.02(9)
$\langle\pi_{11}^2\rangle / \langle\tilde{\pi}_6^2\rangle$	29(8)	6.9(6)	3.5(1)	1.66(5)	1.03(7)
$\langle\tilde{\sigma}^2\rangle / \langle\tilde{\pi}_{16}^2\rangle$	156(226)	7.6(7)	3.6(2)	1.70(6)	1.02(9)
P_3	−0.059(1)	−0.061(2)	−0.058(2)	−0.056(3)	−0.057(3)

TABLE VI. The ratios of hypercube meson field fluctuations at $\beta = 5.25$. The notation $\langle\sigma^2\rangle_c$ means $\langle\sigma^2\rangle - \langle\sigma\rangle^2$.

m	0.100	0.075	0.050	0.025	0.0125	0.00
$\langle\pi_{16}^2\rangle / \langle\sigma^2\rangle_c$	2.3(2)	1.35(1)	1.16(2)	1.04(1)	1.01(1)	1.000(7)
$\langle\pi_6^2\rangle / \langle\tilde{\pi}_{11}^2\rangle$	2.1(2)	1.55(3)	1.24(3)	1.06(3)	1.01(1)	0.994(10)
$\langle\pi_7^2\rangle / \langle\tilde{\pi}_{10}^2\rangle$	2.0(2)	1.58(3)	1.25(3)	1.06(3)	1.02(2)	1.00(16)
$\langle\pi_8^2\rangle / \langle\tilde{\pi}_9^2\rangle$	2.6(1)	1.56(3)	1.24(3)	1.06(3)	1.02(3)	0.971(20)
$\langle\pi_9^2\rangle / \langle\tilde{\pi}_8^2\rangle$	2.8(2)	1.55(3)	1.24(3)	1.06(3)	1.01(3)	0.984(21)
$\langle\pi_{10}^2\rangle / \langle\tilde{\pi}_7^2\rangle$	2.7(5)	1.59(3)	1.25(3)	1.06(3)	1.02(2)	0.998(17)
$\langle\pi_{11}^2\rangle / \langle\tilde{\pi}_6^2\rangle$	2.5(6)	1.56(3)	1.24(3)	1.06(3)	1.01(2)	0.994(17)
$\langle\tilde{\sigma}^2\rangle / \langle\tilde{\pi}_{16}^2\rangle$	2.6(6)	1.57(4)	1.25(3)	1.06(3)	1.02(2)	1.001(17)
P_3	−0.054(2)	−0.052(1)	−0.053(2)	−0.051(2)	−0.051(1)	−0.051(2)

TABLE VII. Results for the odd-even meson fields at $\beta = 5.10$. The notation $\langle\sigma^2\rangle_c$ means $\langle\sigma^2\rangle - \langle\sigma\rangle^2$; similarly, the notation $\langle\pi^2\sigma\rangle_c$ means $\langle\pi^2\sigma\rangle - \langle\pi^2\rangle\langle\sigma\rangle$; the notation $\langle\pi^2\sigma\rangle_{\text{conn}}$ means $\left\langle \langle\pi^2\sigma\rangle_f - \langle\pi^2\rangle_f \langle\sigma\rangle_f \right\rangle_g$.

m	0.100	0.075	0.050	0.025	0.00
$\langle\sigma\rangle$	1.07(1)	0.977(7)	0.850(7)	0.589(9)	0.215(18)
$\langle\sigma^2\rangle_c$	0.10(1)	0.059(2)	0.054(5)	0.058(6)	0.056(8)
$\langle\pi^2\rangle_c$	0.354(5)	0.319(6)	0.282(5)	0.233(8)	0.206(6)
$\langle\pi^2\sigma\rangle$	0.233(3)	0.194(4)	0.143(2)	0.080(3)	0.038(3)
$\langle\pi^2\rangle / \langle\sigma^2\rangle_c$	3.4(1)	5.4(4)	5.2(4)	4.0(5)	4.2(5)
$\langle\pi^2\sigma\rangle_{\text{conn}}$	−0.147(3)	−0.125(4)	−0.096(3)	−0.055(5)	
$\langle\pi^2\sigma\rangle_c$	−0.146(7)	−0.118(7)	−0.097(5)	−0.057(6)	
P_3	−0.39(1)	−0.37(2)	−0.40(4)	−0.42(3)	−0.44(3)

TABLE VIII. Results for the odd-even meson fields at $\beta = 5.25$. The notation is the same as in Table VII.

m	0.100	0.075	0.050	0.025	0.0125	0.00
$\langle\sigma\rangle$	0.77(1)	0.56(4)	0.39(1)	0.20(1)	0.104(5)	0.009(8)
$\langle\sigma^2\rangle_c$	0.014(2)	0.083(2)	0.115(3)	0.153(4)	0.155(2)	0.157(3)
$\langle\pi^2\rangle$	0.234(2)	0.195(3)	0.178(4)	0.177(5)	0.159(2)	0.155(3)
$\langle\pi^2\sigma\rangle$	0.115(2)	0.071(2)	0.045(2)	0.022(1)	0.011(2)	0.007(1)
$\langle\pi^2\rangle / \langle\sigma^2\rangle_c$	16.3(2.4)	2.34(9)	1.55(7)	1.12(6)	1.03(3)	0.98(3)
$\langle\pi^2\sigma\rangle_{\text{conn}}$	−0.066(2)	−0.039(1)	−0.026(1)	−0.014(1)	−0.0061(2)	
$\langle\pi^2\sigma\rangle_c$	−0.065(3)	−0.038(8)	−0.024(3)	−0.013(2)	−0.005(2)	
P_3	−0.362(9)	−0.34(1)	−0.36(2)	−0.39(3)	−0.37(1)	−0.36(1)

Tables V and VI. Again a Padé extrapolation to zero mass is shown. It is apparent from this extrapolation that within errors, all ratios of fluctuations approach one at both high and low temperature with the exception of the ratio $\langle\pi_{16}^2\rangle / (\langle\sigma^2\rangle - \langle\sigma\rangle^2)$. This ratio differs significantly from one at low temperature, but is consistent with one at high temperature. On the other hand, the correlation P_3 is small and apparently changes very little from low to high temperature.

These results for the correlation P_3 from the hypercube definition of the fields may be compared with the results from the even-odd construction in Tables VII and VIII, where a few other expectation values are also listed. It is apparent that P_3 is much larger in magnitude, but again little changed from low to high temperature. Our results for other powers of the fields change little from low to high temperature.

Further discussion of these results is deferred to the concluding section.

V. THREE-DIMENSIONAL U(1) SIMULATION

Since it was not obvious what an action with the potential (3) should give for the ratio of fluctuations of the π and σ fields (7) and the Mexican-hat statistic (6), and because mean-field theory is particularly unreliable for a strongly coupled linear σ model, we carried out a simulation of the closely related lattice U(1) chiral model at finite temperature. The purpose of this study is to determine the same expectation values in the U(1) model, so the results can be compared with what we obtain from full QCD. For simplicity, we use a three-dimensional model, corresponding to a high-temperature approximation. The three-dimensional U(1) model (X-Y model) has a long history [18].

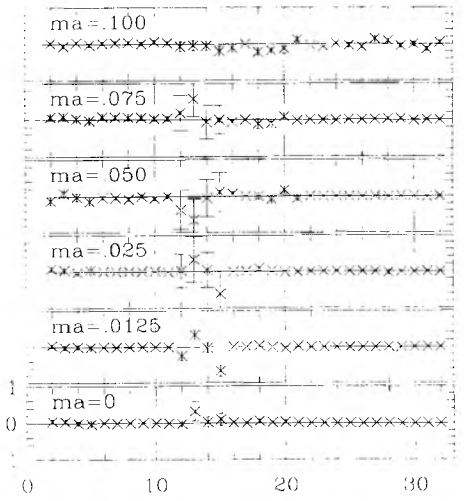

FIG. 2. Same as Fig. 1, except at $\beta = 5.25$.

On a regular periodic lattice, we introduce a U(1) field on each site x. The Hamiltonian is

$$H = \left(\sum_{(x,y)} [1 - U(x) \cdot U^\dagger(y)] + m \sum_x [1 - U(x)] \right) + \text{H.c.}, \tag{72}$$

where (x, y) refers to unique nearest neighbors. A symmetry-breaking term has been included. We define the meson fields through

$$U = \sigma + i\pi. \tag{73}$$

The finite-temperature partition function is given by

$$Z = \int (dU) e^{-\beta H}, \tag{74}$$

where, as usual, $\beta = J/T$ in terms of the coupling constant J and temperature T. At $m = 0$ this model is known to have a continuous chiral-symmetry-restoring phase transition, which can be located by measuring the order parameter $\sigma = \text{Re}(U)$ as a function of inverse temperature β and symmetry-breaking parameter m, when m is not too small. As we shall see, it can also be located from the ratio of chiral fluctuations of π and σ.

On a 10^3 lattice for each β and m we performed 2000 warmup Metropolis iterations followed by 10 000 iterations to make 200 independent measurements. For $m = 0.001$ we performed 50 000 iterations to make 1000 measurements. The averaged results are shown in the Table IX. Also shown is an extrapolation of the results to zero mass. The extrapolation is subtle, since on a finite volume there is no symmetry breaking at zero mass. A proper extrapolation would take the large volume limit first and then take the zero mass limit, using a form con-

sistent with chiral perturbation theory, [19]. For present purposes we chose the expedient of omitting the smallest mass point in order to carry out the extrapolation of the potentially symmetry-sensitive quantities, namely, σ and the fluctuation ratio $\langle\pi^2\rangle / \langle\sigma^2\rangle_c$. From the extrapolation we can see from $\langle\sigma\rangle$ that the critical point is between β =0.44 and 0.46, consistent with previous results [18]. We note that the fluctuation ratio tends to one at high temperature, but differs from one at low temperature, just as in QCD. The Gaussian model would also be expected to yield a ratio of one. Thus the high-temperature result merely reflects the restoration of chiral symmetry and evidently does not distinguish between a Gaussian model and a Mexican-hat model. By contrast, the correlation function P_3 stays negative with no dramatic dependence on m in both the broken-symmetry and restored-symmetry phases, whereas we would expect it to drop to nearly zero in the Gaussian model. Note that the values

TABLE IX. Chiral model results. The zero mass values were obtained by extrapolation as described in the text. The notation $\langle\sigma^2\rangle_c$ means $\langle\sigma^2\rangle - \langle\sigma\rangle^2$.

β	m	σ	π	$\langle\pi^2\rangle / \langle\sigma^2\rangle_c$	P_3
0.44	0.04	0.32(5)	0.026(50)	1.15(7)	−0.48(1)
0.44	0.03	0.29(5)	−0.000(50)	1.12(2)	−0.49(3)
0.44	0.02	0.24(5)	0.020(50)	1.08(3)	−0.49(4)
0.44	0.01	0.11(5)	0.006(50)	1.02(3)	−0.51(3)
0.44	0.005	0.05(5)	0.010(50)	1.01(1)	−0.50(8)
0.44	0.001	0.02(2)	0.010(22)	1.00(2)	−0.50(3)
0.44	0	0.01(2)	0.009(20)	0.99(1)	−0.50(4)
0.45	0.04	0.37(4)	0.014(50)	1.21(6)	−0.48(2)
0.45	0.03	0.35(4)	0.012(50)	1.19(1)	−0.48(2)
0.45	0.02	0.30(5)	−0.007(50)	1.13(5)	−0.49(2)
0.45	0.01	0.17(5)	0.004(50)	1.04(5)	−0.48(3)
0.45	0.005	0.08(5)	0.012(50)	1.02(2)	−0.52(6)
0.45	0.001	0.02(5)	0.004(50)	0.998(6)	−0.45(3)
0.45	0	0.05(4)	0.001(50)	0.991(6)	−0.46(4)
0.46	0.04	0.43(4)	−0.026(48)	1.29(7)	−0.47(1)
0.46	0.03	0.41(4)	−0.008(48)	1.27(6)	−0.47(1)
0.46	0.02	0.34(5)	0.014(49)	1.17(4)	−0.48(2)
0.46	0.01	0.26(5)	−0.003(50)	1.11(5)	−0.49(1)
0.46	0.005	0.22(5)	0.060(50)	1.07(3)	−0.50(3)
0.46	0.001	0.02(2)	−0.013(22)	1.01(7)	−0.49(2)
0.46	0	0.21(4)	0.01(2)	1.05(3)	−0.49(3)
0.47	0.04	0.47(4)	0.009(48)	1.38(2)	−0.46(1)
0.47	0.03	0.42(4)	−0.006(48)	1.31(1)	−0.47(1)
0.47	0.02	0.41(4)	0.020(49)	1.29(1)	−0.47(1)
0.47	0.01	0.31(5)	0.074(49)	1.16(1)	−0.49(2)
0.47	0.005	0.21(5)	0.030(50)	1.06(1)	−0.49(2)
0.47	0.001	0.03(5)	−0.050(50)	1.00(3)	−0.51(3)
0.47	0	0.22(4)	−0.02(5)	1.05(1)	−0.50(2)
0.48	0.04	0.50(4)	0.008(47)	1.46(2)	−0.45(1)
0.48	0.03	0.49(4)	0.025(47)	1.44(1)	−0.45(2)
0.48	0.02	0.46(4)	−0.063(48)	1.38(1)	−0.46(1)
0.48	0.01	0.41(4)	−0.055(49)	1.30(1)	−0.48(1)
0.48	0.005	0.33(4)	0.014(50)	1.23(4)	−0.49(2)
0.48	0.001	0.10(2)	−0.006(22)	1.01(1)	−0.49(1)
0.48	0	0.34(3)	−0.008(30)	1.21(2)	−0.49(1)
0.50	0.04	0.55(4)	0.027(46)	1.61(1)	−0.44(2)
0.50	0.03	0.54(4)	−0.008(47)	1.58(1)	−0.44(1)
0.50	0.02	0.51(4)	0.011(47)	1.52(2)	−0.45(2)
0.50	0.01	0.40(4)	0.015(49)	1.31(1)	−0.48(3)
0.50	0.005	0.32(5)	−0.041(50)	1.25(2)	−0.51(4)
0.50	0.001	0.10(2)	−0.008(22)	1.02(3)	−0.48(4)
0.50	0	0.33(5)	0.002(20)	1.20(2)	−0.49(2)

are close to those we obtained from full QCD with the odd-even definition of the chiral fields.

VI. DISCUSSION

Our results can be explained simply according to the following model.

(1) Parity invariance and the vectorlike symmetries hold for all masses and both temperatures. These conditions require

$$\langle \pi_a \rangle = \langle \tilde{\pi}_a \rangle = 0 \quad \text{for } a = 2,3,\ldots,16,$$
$$\langle \tilde{\sigma} \rangle = 0.$$

(2) The surviving continuous U(1) subgroup of chiral SU(4)×SU(4) is spontaneously broken at low temperature and restored at high temperature.

(3) All discrete axial symmetries are broken spontaneously at low temperature.

(4) The local effective potential resembles that of a nonlinear σ model at both low and high temperature with no appreciable change.

Parity alone would not account for the vanishing of all but $\langle \sigma \rangle$, regardless of mass and temperature. Therefore, we need the vectorlike symmetries. If any of the discrete axial symmetries were valid at low temperature, we would have $\langle \sigma \rangle = 0$ in the chiral limit, which is not found. The vanishing of $\langle \sigma \rangle$ does not by itself distinguish a restoration of the axial-like symmetries at high temperature from a restoration of the U(1) symmetry. However, the observation of chiral multiplets [3, 4] argues in favor of a restoration of the U(1) symmetry. Our results are of course consistent with a restoration of the discrete axial symmetries at high temperature, but they do not require it.

We turn now to our main result, namely the value of the Mexican-hat statistic P_3. As expected, the hypercube value is considerably smaller than the odd-even value. The ratio is about 1:7.5 at low temperature and 1:7 at high temperature, quite close to our estimate (70). Let us check our two assumptions that led to this estimate, namely, whether the color disconnected terms are negligible. In Tables VII and VIII are shown values for the contribution to the quantity $\left\langle \langle \pi^2 \sigma \rangle_f - \langle \pi^2 \rangle_f \langle \sigma \rangle_f \right\rangle_g$ coming from connected diagrams and values $\langle \pi^2 \sigma \rangle - \langle \pi^2 \rangle \langle \sigma \rangle$ for both connected and disconnected contributions to the same quantity. We see that the difference is indeed small, suggesting that the contribution of the disconnected diagrams is at most as large as the statistical error. Therefore, our approximation is justified.

For this reason we believe that, but for the suppression resulting from a coarse lattice, our results for P_3 would be equally large with both definitions. The odd-even value for P_3 is approximately -0.4 with no dramatic dependence on m in both the broken-symmetry and restored-symmetry phases, whereas in the Gaussian model we would expect it to drop to nearly zero with increasing temperature. Putting this result together with the mean-field theory analysis of the Appendix and the U(1) chiral model simulation, we find that only the strongly coupled Mexican-hat potential and the essentially equivalent nonlinear σ model are consistent with the QCD simulation.

Consequently, we find that our results for P_3 and the rough equality of the fluctuations of the meson fields at low and high temperatures shown in Tables VII and VIII favor an effective nonlinear U(1) chiral model that changes little across the phase transition. Further work is needed to establish whether these results hold in the continuum limit. It would also be interesting to extend the comparison between the actual and effective models to measurements of screening lengths.

ACKNOWLEDGMENTS

We would like to thank Doug Toussaint for helpful discussions in the initial stages of this work and Keh-Fei Liu for assistance in obtaining part of the necessary computer time. This work was supported in part by Grant No. PHY-9008482 of the National Science Foundation. Computations were carried out in part on an IBM 3090/600S at the University of Utah Supercomputer Institute, on a Cray Y-MP at the San Diego Supercomputer Center, on an IBM 3090/600J at the University of Kentucky, on a Cray Y/MP at Florida State University, and for the chiral model and on IBM RS-6000/320 work stations at the University of Utah. The authors wish to express their gratitude to these centers for providing computer time.

APPENDIX: MEAN-FIELD LINEAR σ MODEL

We consider an SU(2) lattice linear σ model in the high-temperature approximation. Write the action as

$$H(\pi,\sigma) = \sum_{r,\mu} [(\pi_r - \pi_{r+\mu})^2/2a^2 + (\sigma_r - \sigma_{r+\mu})^2/2a^2] + \sum_r V(\pi_r, \sigma_r),$$

where r ranges over the sites of a cubic three-dimensional lattice and

$$V(\pi,\sigma) = \lambda(\pi^2 + \sigma^2 \pm f_\pi^2)^2 - \mu\sigma.$$

We want to compute expectation values on the Gibbs ensemble

$$Z = \int \prod_r d\sigma_r d\pi_r \exp[-\beta H(\pi,\sigma)].$$

With the negative sign (Mexican-hat shape) the mean-field approximation is not good for strong coupling, since the dominant field configurations tend to form spin waves and vortices with strong correlations in angle between neighbors. Thus the global mean value is a poor approximation to the actual value of the neighbor. However, for weak coupling and for strong coupling with the positive sign (bowl shape) we expect to do better. In a mean-field approximation we consider the single-site partition function

$$Z_{ss} = \int d\sigma\, d\pi \exp[-\beta H_{ss}(\pi,\sigma)],$$

where

$$H_{ss}(\pi,\sigma) = 3(\pi-\bar{\pi})^2/2a^2 + 3(\sigma-\bar{\sigma})^2/2a^2 + V(\pi,\sigma),$$

where $\bar{\pi}$ is the mean value of π and $\bar{\sigma}$ is the mean value of σ. Now $\bar{\pi}=0$ and for small μ, $\bar{\sigma}\propto\mu$, so

$$H_{ss}(\pi,\sigma) = \lambda(\pi^2+\sigma^2)^2 + (3/2a^2 \pm 2\lambda f_\pi^2)(\pi^2+\sigma^2) - \alpha\mu\sigma + \text{const.}$$

So with a redefinition of constants, and a rescaling of the fields, the mean-field action takes a form resembling the bowl potential:

$$H_{ss}(\pi,\sigma) = \lambda'(\pi^2+\sigma^2+1)^2 - \mu'\sigma + \text{const},$$

where

$$\lambda' = \lambda\left(\frac{3}{4a^2\lambda} \pm f_\pi^2\right)^2,$$

$$\mu' = \alpha\mu\sqrt{\frac{3}{4a^2\lambda} \pm f_\pi^2}.$$

Notice that this form of the potential is inappropriate for strong coupling with the minus sign (hat) choice, since μ' would become imaginary. In that case we must use

$$H_{ss}(\pi,\sigma) = \lambda'(\pi^2+\sigma^2-1)^2 - \mu'\sigma + \text{const}$$

with a redefinition of μ' that takes the square root of a positive quantity.

We then analyze the expectation value of P_3 on the single site action in the limit $\mu'\to 0$. We use polar coordinates $\pi = t\sin\theta$, $\sigma = t\cos\theta$, and must evaluate

$$\langle\pi^2\sigma\rangle \to -\mu' N\int_0^\infty t\,dt\int_0^{2\pi} d\theta\, t^4\sin^2\theta\cos^2\theta\exp[-\lambda'(t^2\pm 1)^2],$$

$$\langle\pi^2\rangle \to N\int_0^\infty t\,dt\int_0^{2\pi} d\theta\, t^2\sin^2\theta\exp[-\lambda'(t^2\pm 1)^2],$$

$$\langle\sigma\rangle \to -\mu' N\int_0^\infty t\,dt\int_0^{2\pi} d\theta\, t^2\cos^2\theta\exp[-\lambda'(t^2\pm 1)^2],$$

where

$$N^{-1} = \int_0^\infty t\,dt\int_0^{2\pi} d\theta\,\exp[-\lambda'(t^2\pm 1)^2].$$

Simplifying, we have

$$P_3(0) = \lim_{\tilde{\mu}\to 0}\frac{\langle\pi^2\sigma\rangle}{\langle\pi^2\rangle\langle\sigma\rangle} - 1 = \frac{\langle t^4\rangle\langle 1\rangle}{2\langle t^2\rangle^2} - 1,$$

where

$$\langle t^n\rangle = \int_0^\infty dt\, t^{n+1}\exp[-\lambda'(t^2+s)^2],$$

with $s=\pm 1$. In Table X we give a sampling of results for the expectation value $P_3(0)$ for either choice of the sign s. We see that in the limit $\tilde{\lambda}\to 0$ both distributions ($s=\pm 1$) give the same value. However, with $s=1$ the result is never less than -0.22.

TABLE X. Expected values of the Mexican-hat statistic for the linear σ model with two choices for the sign s. The minus sign gives the Mexican-hat form and the plus sign gives the bowl form.

λ'	s	$P_3(0)$	s	$P_3(0)$
8.00	−1	−0.46877	1	−0.04150
4.00	−1	−0.43911	1	−0.06394
2.00	−1	−0.39507	1	−0.08978
1.00	−1	−0.34867	1	−0.11572
0.50	−1	−0.31010	1	−0.13901
0.10	−1	−0.25620	1	−0.17740
0.02	−1	−0.23277	1	−0.19733
0.001	−1	−0.21867	1	−0.21072

[1] L. Dolan and R. Jackiw, Phys. Rev. D **9**, 3320 (1974).

[2] See the review by F. Karsch, in *Quark-Gluon Plasma*, edited by R.C. Hwa (World Scientific, Singapore, 1991).

[3] C.E. DeTar and J.B. Kogut, Phys. Rev. Lett. **59**, 399 (1987); Phys. Rev. D **36**, 2828 (1987).

[4] S. Gottlieb, W. Liu, D. Toussaint, R.L. Renkin, and R.L. Sugar, Phys. Rev. Lett. **59**, 1881 (1987); A. Gocksch, P. Rossi, and U. Heller, Phys. Lett. B **205**, 334 (1988).

[5] J. Kogut, M. Stone, H.W. Wyld, S.H. Shenker, J. Shigemitsu, and D.K. Sinclair, Nucl. Phys. **B225**, 326 (1983).

[6] E. Laermann, R. Altmeyer, K.D. Born, M. Göckeler, R. Horsley, W. Ibes, T.F. Walsh, and P.M. Zerwas, in *Lattice '90*, Proceedings of the International Symposium, Tallahassee, Florida, 1990, edited by U. M. Heller, A. D. Kennedy, and S. Sanielevici [Nucl. Phys. B (Proc. Suppl.) **20**, 380 (1991)].

[7] T.H.R. Skyrme, Nucl. Phys. **31**, 556 (1962).

[8] T.W.B. Kibble, J. Phys. A **9**, 1387 (1976); T.A. DeGrand, Phys. Rev. D **30**, 2001 (1984); J. Ellis and H. Kowalski, Phys. Lett. B **214**, 161 (1988); CERN Report No. CERN-TH-5316/89, 1989 (unpublished); A.H. Mueller, in *Quark Matter '88*, Proceedings of the 7th International Conference on Ultrarelativistic Nucleus-Nucleus Collisions, Lenox, Massachusetts, 1988, edited by G. Baym, P. Braun-Munzinger, and S. Nagamiya [Nucl. Phys. **A498** (1989)].

[9] C.E. DeTar, Phys. Rev. D **42**, 224 (1990).

[10] S. Gavin, M. Gyulassy, M. Plumer, and R. Venugopalan, Phys. Lett. B **234**, 175 (1990)
[11] For two recent examples, see C.E. DeTar and T. Kunihiro, Phys. Rev. D **39**, 2805 (1989); A. Gocksch, Phys. Rev. Lett. **67**, 1701 (1991).
[12] N. Kawamoto and J. Smit, Nucl. Phys. **B192**, 100 (1981).
[13] H. Kluberg-Stern, A. Morel, O. Napoly, and B. Petersson, Nucl. Phys. **B220**, 447 (1983).
[14] J. Kogut, M. Stone, H.W. Wyld, S.H. Shenker, J. Shigemitsu, and D.K. Sinclair, Nucl. Phys. **B225** [FS9], 326 (1983).
[15] M. Gell-Mann and M. Lévy, Nuovo Cimento **16**, 705 (1960); J. Schwinger, Ann. Phys. (N.Y.) **2**, 407 (1958).
[16] J.B. Kogut and D.K. Sinclair, Nucl. Phys. **B280**, 625 (1987).
[17] M.F.L. Golterman, Nucl. Phys. **B273**, 663 (1986).
[18] See G. Kohring, R.E. Shrock, and P. Wills, Phys. Rev. Lett. **57**, 1358 (1986), and references therein.
[19] A. Hasenfratz *et al.*, Nucl. Phys. **B356**, 332 (1991).